

A Framework for Automated Quantification of Calcified Coronary Artery from Intravascular Optical Coherence Tomography Images

Yiqing Liu

*Institute for Medical Engineering and
Science
Massachusetts Institute of Technology
Cambridge, USA
lyiqing@mit.edu*

Farhad R. Nezami

*Division of Cardiac Surgery
Brigham and Women's Hospital
Boston, USA
frikhtegarnezami@bwh.harvard.edu*

Elazer R. Edelman

*Institute for Medical Engineering and
Science
Massachusetts Institute of Technology
Cambridge, USA
ere@mit.edu*

Abstract—Intravascular Optical Coherence Tomography (OCT) has emerged as a powerful imaging modality for assessing the morphological characteristics of coronary arteries. Quantification of calcified coronary arteries from OCT images is crucial for evaluating the severity and progression of coronary artery disease. However, in current practice, OCT images are interpreted manually which is time-consuming, subjective, and prone to inter- and intra-observer variability. To address these limitations, we propose a framework for automated quantification of calcified coronary arteries from OCT images. By leveraging deep learning techniques, the proposed framework automatically segments lumen and calcified plaque from OCT images. Subsequently, comprehensive morphological analysis of lumen and calcified plaque is performed using advanced image processing algorithms, allowing for retrieval of various dimensions of corresponding structures. Following that, essential shape measurements are derived to ensure adequate characterization of calcified coronary arteries. The efficacy of the proposed framework was validated on a clinical dataset. Extensive experiments have demonstrated high accuracy and consistency of quantitative results estimated by the proposed framework against manual analysis with relative errors of less than 10%. The proposed framework holds great potential to extend its application to characterization of other non-calcified plaques and arteries, aiding in clinical intervention and translational research using OCT.

Keywords—*intravascular OCT, coronary artery calcification, quantitative analysis*

I. INTRODUCTION

Coronary artery calcification is concomitant with the development of advanced atherosclerosis [1]. Both the extent and pattern of calcification provide valuable information about the progression and severity of disease [2]. Calcification impairs coronary blood flow and poses challenges to intervention procedures by inhibiting optimal device deployment, poorly portending for complications and stent failure [3]. Thus, quantitative assessment of coronary calcification plays an indispensable role in clinical risk stratification, monitoring disease progression, guiding therapeutic interventions, and evaluating treatment efficacy.

Intravascular optical coherence tomography (OCT) has emerged as a powerful imaging modality for assessing morphological characteristics of coronary artery. It provides exceptionally high-resolution cross-sectional images of the coronary arteries which allows for identification and characterization of calcified plaques with superior clarity

compared to other imaging modalities [4]. OCT is therefore increasingly leveraged for guiding interventions, ensuring accurate deployment and optimizing outcomes. However, in current practice the extraction and interpretation of OCT features are predominantly performed by trained experts. Due to large volume of image frames in OCT pullbacks (ranging from 300 to 500 frames per pullback), this manual reviewing process is labor-intensive, time-consuming, and subject to significant inter- and intra-observer variability. There is a recognized need for automated image analysis and annotation methods to improve efficiency, standardization, and accuracy in interpreting OCT images.

Recent years have witnessed a surge of research dedicated to leveraging deep learning techniques for automated plaque characterization from OCT images. Athanasiou, et al. [5] developed a 45-layer convolutional neural network (CNN) to detect calcified, lipid, fibrous, mixed, non-visible, and non-pathological tissue within arterial wall. Kolluru, et al. [6] used a 7-layer CNN to classify A-lines of different plaques from OCT images. In recent studies, Gessert, et al. [7] employed state-of-the-art deep learning models to directly classify plaques from the images. Abdolmanafi et al. [8] utilized pretrained, end-to-end fully convolution neural network for segmentation of calcified, fibrotic, infiltrated macrophage and neovascularized lesions. Avital et al. [9] applied U-Net to recognize calcifications from OCT images. Gharaibeh et al. [10] built a platform for automatic segmentation of lumen and calcified plaque followed with semiautomatic measurements of calcified arc and thickness from OCT images using image processing techniques.

While the preceding literature review showcased notable advancements in automated OCT analysis, it is important to acknowledge that the majority of the studies have primarily focused on plaque classification and segmentation by embedding various existing CNN architectures. The automatic quantification of calcified arteries from OCT images is still underexplored.

This paper presents a comprehensive framework for automated quantification of calcified artery from OCT images. The proposed framework begins by utilizing our previously developed Transformer-based segmentation model to identify lumen and calcified plaque regions. The segmented masks are then subjected to morphological analysis, enabling direct measurement of various luminal and plaque dimensions. Following that, essential shape measurements are

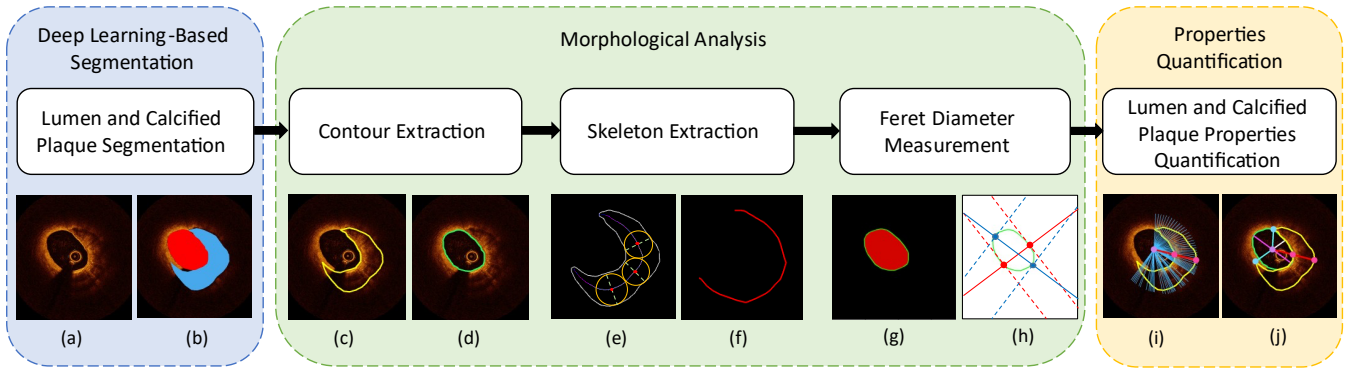


Fig. 1. Framework overview. (a) Original OCT image. (b) Segmented lumen and calcified plaque. (c) Calcified plaque contour. (d) Lumen contour. (e) Skeleton extraction process. (f) Skeleton of calcified plaque. (g) Convex hull of lumen. (h) Feret diameter of lumen. (i) Calcified plaque thickness measurement. (j) Lumen and calcified plaque properties quantification.

derived to adequately characterize calcified coronary arteries. The proposed framework achieved promising performance when evaluated on clinical dataset in comparison to manual annotation and quantification.

II. METHODOLOGY

The framework (Fig. 1) involves: deep learning-based OCT segmentation; morphological analysis of lumen and calcified plaque regions; and quantification of critical properties.

A. Deep Learning-Based Segmentation

Intravascular OCT images, given their highly contextual nature, require understanding of spatial relationships and structures to accurately identify and quantify calcified coronary arteries. They capture not only detailed information about the composition of the vessel but also provide contextual cues regarding the intricate relationships between lesions, lumen, arterial wall, and various artifacts (i.e., guidewire, residual blood, etc.). Existing methods to segment atherosclerotic plaques from OCT images have been predominantly fueled by integration of CNNs. Despite their success in capturing local features, the limited receptive field inherent to convolution operation restricts their performance in capturing global contexts. In contrast, Transformer architecture [11] has shown promise in capturing global context and long-range dependencies in images by leveraging self-attention mechanisms. Transformers are particularly beneficial when it comes to identifying calcified coronary arteries where contextual information plays a crucial role. In this framework, our previously developed Transformer-based encoder-decoder model [12] was used to conduct end-to-end, semantic segmentation of OCT images. Given an original OCT image (Fig. 1(a)), the output of the model was the segmented lumen and calcified plaque covered with red and blue masks, respectively (Fig. 1(b)).

B. Morphological Analysis

The luminal and calcified plaque properties were measured in pixels from the segmented mask. The contours of both lumen and calcified plaque were traced (Fig. 1(c) and Fig. 1(d)) and the skeleton of calcified plaque (Fig. 1(f)) was constructed by identifying the centroids of circles tangent to the calcified plaque contours (Fig. 1(e)). The Feret diameter (also known as caliper diameter), referring to the distance between two parallel lines that can be drawn perpendicular to each other and touch the boundary of region of interest, can then be measured (Fig. 1(h)). This is an essential metric for

characterizing the size, shape, and spatial extent of objects in the image.

Table 1 illustrates the pseudocode for the algorithm designed to calculate the maximum and minimum Feret diameter denoted as F_{max} and F_{min} . The convex hull of the lumen was determined as the smallest convex polygon that encompassed all the lumen boundary points (Fig. 1(g)). By iterating over all the edge points P_i ($i=1,2,\dots,n$), all the Euclidean distances d between each pair of edge points on the convex hull were calculated to obtain the maximum and minimum Feret diameter (blue and red solid lines in Fig. 1(h)). Similarly, the Feret diameter of calcified plaque was also measured.

TABLE I. FERET DIAMETER CALCULATION ALGORITHM

Algorithm 1 Calculate Feret diameter

Input: Segmented mask I containing the region of interest
Output: F_{max}, F_{min}

- 1: compute the convex hull of the boundary pixels $H = \{(x_i, y_i), i = 1, 2, \dots, n\}$
- 2: initialize $F_{max} = 0, F_{min} = \infty$
- 3: **for** $P_i = (x_i, y_i)$ in H **do**
- 4: **for** $P_{i+1} = (x_{i+1}, y_{i+1})$ in H **do**
- 5: $d = \sqrt{(y_i - y_{i+1})^2 + (x_i - x_{i+1})^2}$
- 6: $F_{max} = d$
- 7: **if** $F_{max} < F_{min}$ **then**
- 8: $F_{min} = F_{max}$
- 9: **end**
- 10: **end**
- 11: **end**
- 12: **return** F_{max}, F_{min}

C. Properties Calculation

The prior morphological analysis allows for measuring the basic geometric dimensions of luminal and calcified plaque. Several essential shape descriptors were further calculated to ensure adequate characterization of calcified coronary artery for comprehensive clinical assessment. Table 2 summarizes all the properties related to lumen and calcified plaque.

The luminal and plaque area and perimeter were derived from the enclosed area and length of contours of corresponding regions. By projecting a straight line from the centroid of lumen, the intersection points between this line and lumen contour were obtained. Considering the irregular shape of lumen, the minimum diameter d_{min} (white line in Fig. 1(j)),

maximum diameter d_{max} (purple line in Fig. 1(j)), and mean diameter were calculated by comparing the Euclidean distances between each pair of intersection points. Similarly, the intersection points between the line and plaque contour were obtained (blue lines in Fig. 1(i)). The calcified plaque thickness was determined by measuring the maximum Euclidean distance between each pair of intersection points (pink line in Fig. 1(i)). The calcified plaque arc was quantified by computing the angle between two lines connecting the centroid of the lumen and the two endpoints of the calcified plaque skeleton (blue lines in Fig. 1(j)).

TABLE II. LUMEN AND CALCIFIED PLAQUE PROPERTIES

Lumen Properties	Calcified Plaque Properties
Area	Arc
Perimeter	Thickness
Mean diameter	Area
Circularity	Perimeter
Convexity	Circularity
Solidity	Convexity
Asymmetry	Solidity
Elongation	Elongation

Apart from the above geometric properties, several shape descriptors were further calculated to characterize the lumen and calcified plaque appearance from different perspectives, including circularity, convexity, solidity, elongation, and asymmetry ((1)-(5)).

$$Circularity = \frac{4\pi \times Area}{(Convex Perimeter)^2} \quad (1)$$

$$Convexity = \frac{Convex Perimeter}{Perimeter} \quad (2)$$

$$Solidity = \frac{Area}{Convex Area} \quad (3)$$

$$Elongation = \frac{F_{min}}{F_{max}} \quad (4)$$

$$Asymmetry = \frac{d_{min}}{d_{max}} \quad (5)$$

III. EXPERIMENTAL VALIDATION

The proposed framework was validated on a clinical OCT dataset, demonstrating its promising performance when compared to manual annotation and quantification.

A. Dataset

The dataset consisted of 2000 image frames from pullbacks of 60 patients who were potential candidates for intravascular lithotripsy (IVL, Shockwave, CA). Such a cohort is more desirable to challenge our platform as IVL-candidate plaques are majorly calcium-heavy. In total 1800 images from 50 pullbacks and 200 images from 10 pullbacks were randomly selected from the dataset for training and testing of the segmentation model, respectively. The test set was further used to assess the quantification performance. Each image was set of a consistent size of 500×500 pixels. The training and testing sets incorporated coronary arteries distorted to a varying extent and severity of calcification. The ground truth was provided by expert readers through manual annotation of and measurements from OCT images.

B. Experimental Settings

1) *Implementation details*: Data augmentation techniques including geometric transformations and photometric

transformations were applied to the training set to improve the diversity of the image data. The segmentation model was trained using the AdamW optimizer with a weight decay of 0.01. A batch size of 4 was used, and the training process consisted of 120,000 iterations. A learning rate warmup strategy was employed with an initial learning rate of $6e^{-5}$.

2) *Evaluation metrics*: The performance of the segmentation model was evaluated using Intersection over Union (IoU), dice score, precision, and recall, which are defined as follows:

$$IoU = \frac{TP}{TP+FP+FN} \quad (6)$$

$$Dice Score = \frac{2TP}{2TP+FP+FN} \quad (7)$$

$$Precision = \frac{TP}{TP+FP} \quad (8)$$

$$Recall = \frac{TP}{TP+FN} \quad (9)$$

where TP (true positive) and TN (true negative) represent pixels that are correctly classified, and FP (false positive) and FN (false negative) represent pixels that are falsely classified as target region and background, respectively. The quantitative analysis results were evaluated through comparison against manual survey. The relative errors for estimations were computed as indicators of the quantification framework performance as formulated in (10):

$$Relative Error = \frac{|V_{True} - V_{Observed}|}{V_{True}} \quad (10)$$

where V_{True} and $V_{Observed}$ represent true value and observed value respectively.

C. Experimental Analysis

Given the critical role of the OCT segmentation step in the overall quantitative analysis, the segmentation performance was primarily evaluated. Table 3 and Fig. 2 showcases the experimental results for the segmentation of the lumen and calcified plaque. It can be observed that the segmentation model was able to accurately delineate both lumen and calcified plaque with achieved dice score, precision, and recall of over 90%.

TABLE III. QUANTITATIVE OCT SEGMENTATION RESULTS

Target Region	IoU	Dice	Precision	Recall
Lumen	0.9224	0.9578	0.9844	0.9374
Calcified plaque	0.8462	0.9167	0.9120	0.9214

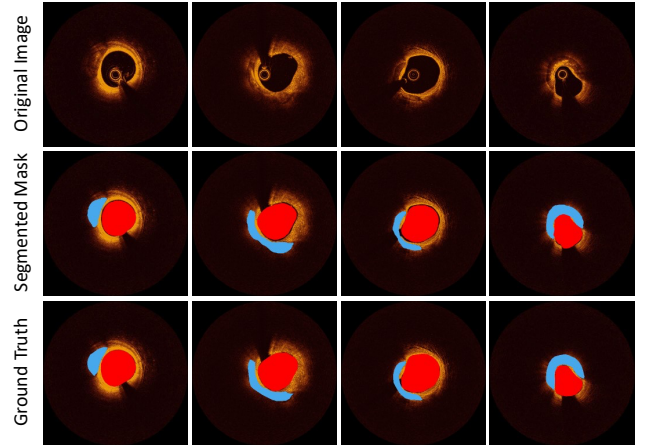


Fig. 2. Example images of segmentation results.

The lumen and calcified plaque quantification results were further evaluated through comparison with manual measurements from images. The calculated relative errors of lumen and calcified plaque are illustrated in Fig. 3 and Fig. 4, respectively. It is noteworthy that the mean relative errors for all the measured luminal and calcified plaque properties were below 10%. Particularly, the proposed framework exhibited higher accuracy and stability in lumen quantification compared to calcified plaque quantification. This observation can be attributed to the superior performance of the model in segmenting lumen in comparison to the calcified plaque. Future research and development efforts should focus on advancing the segmentation algorithms to ensure more accurate and reliable quantification results. In addition to the 2D features extracted in this work, 3D features such as volume-related properties can be further explored in the future.

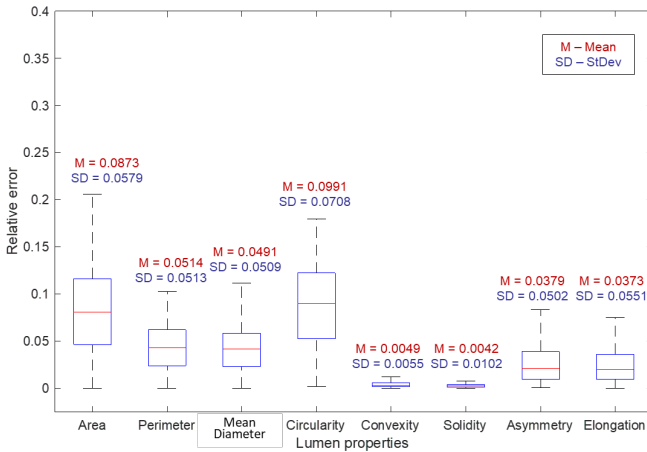


Fig. 3. Boxplot of lumen quantification results.

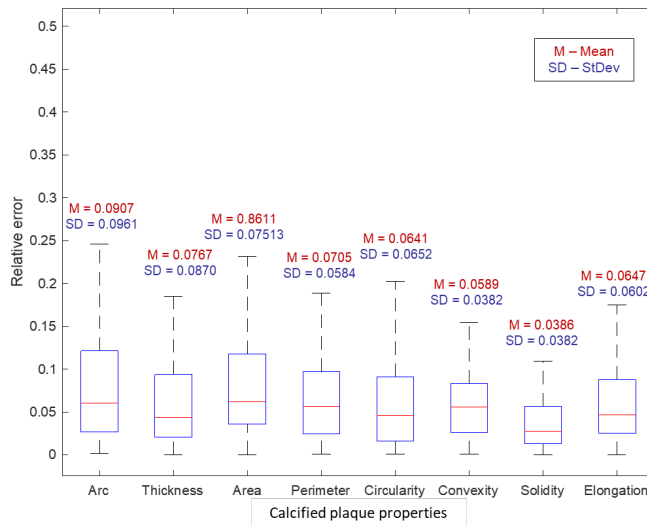


Fig. 4. Boxplot of calcified plaque quantification results.

IV. CONCLUSIONS

The framework presented in this study offers an automated approach for quantifying calcified coronary artery using intravascular OCT images. The effectiveness of the framework in accurately estimating various properties related to the lumen and calcified plaque was successfully demonstrated through rigorous comparison with manual

measurements. Experimental results highlight the significance of segmentation performance in improving the accuracy of subsequent quantifications. The proposed framework can be further developed to encompass the characterization of other atherosclerotic lesions, thereby enhancing its capabilities to support informed clinical decision-making in the diagnosis and treatment of atherosclerosis.

ACKNOWLEDGMENT

The authors gratefully acknowledge Seth Fairfax, Ph.D., Jason Hokama, Ph.D., and Keith D. Dawkins, M.D. from Shockwave Medical Inc. (Santa Clara, CA USA) for providing the data utilized in this research.

REFERENCES

- [1] T. Nakahara, M. R. Dweck, N. Narula, D. Pisapia, J. Narula, and H. W. Strauss, "Coronary artery calcification: From mechanism to molecular imaging," *JACC: Cardiovascular Imaging*, vol. 10, no. 5, pp. 582-593, 2017/05/01/ 2017.
- [2] H. Mori, S. Torii, M. Kutyna, A. Sakamoto, A. V. Finn, and R. Virmani, "Coronary artery calcification and its progression: What does it really mean?," *JACC Cardiovasc Imaging*, vol. 11, no. 1, pp. 127-142, Jan 2018.
- [3] T. J. Ryan, D. P. Faxon, R. M. Gunnar, J. W. Kennedy, S. B. King, F. D. Loop, K. L. Peterson, T. J. Reeves, D. O. Williams, and W. L. Winters, "Guidelines for percutaneous transluminal coronary angioplasty. A report of the american college of cardiology/american heart association task force on assessment of diagnostic and therapeutic cardiovascular procedures (subcommittee on percutaneous transluminal coronary angioplasty)," *Circulation*, vol. 78, no. 2, pp. 486-502, 1988/08/01 1988.
- [4] H. G. Bezerra, M. A. Costa, G. Guagliumi, A. M. Rollins, and D. I. Simon, "Intracoronary optical coherence tomography: A comprehensive review: Clinical and research applications," *JACC: Cardiovascular Interventions*, vol. 2, no. 11, pp. 1035-1046, 2009/11/01/ 2009.
- [5] L. S. Athanasiou, M. L. Olender, J. M. de la Torre Hernandez, E. Ben-Assa, E. R. Edelman, H. K. Hahn, and K. Mori, "A deep learning approach to classify atherosclerosis using intracoronary optical coherence tomography," presented at the Medical Imaging 2019: Computer-Aided Diagnosis, 2019.
- [6] C. Kolluru, D. Prabhu, Y. Gharaibeh, H. Bezerra, G. Guagliumi, and D. Wilson, "Deep neural networks for a-line-based plaque classification in coronary intravascular optical coherence tomography images," *J Med Imaging (Bellingham)*, vol. 5, no. 4, p. 044504, Oct 2018.
- [7] N. Gessert, M. Lutz, M. Heyder, S. Latus, D. M. Leistner, Y. S. Abdelwahed, and A. Schlaefler, "Automatic plaque detection in ivoct pullbacks using convolutional neural networks," *IEEE Trans Med Imaging*, vol. 38, no. 2, pp. 426-434, Feb 2019.
- [8] A. Abdolmanafi, F. Cheriet, L. Duong, R. Ibrahim, and N. Dahdah, "An automatic diagnostic system of coronary artery lesions in kawasaki disease using intravascular optical coherence tomography imaging," *J Biophotonics*, vol. 13, no. 1, p. e201900112, Jan 2020.
- [9] Y. Avital, A. Madar, S. Arnon, and E. Koifman, "Identification of coronary calcifications in optical coherence tomography imaging using deep learning," *Sci Rep*, vol. 11, no. 1, p. 11269, May 28 2021.
- [10] Y. Gharaibeh, D. Prabhu, C. Kolluru, J. Lee, V. Zimin, H. Bezerra, and D. Wilson, "Coronary calcification segmentation in intravascular oct images using deep learning: Application to calcification scoring," *J Med Imaging (Bellingham)*, vol. 6, no. 4, p. 045002, Oct 2019.
- [11] A. Vaswani, N. Shazeer, N. Parmar, J. Uszkoreit, L. Jones, A. N. Gomez, Ł. Kaiser, and I. Polosukhin, "Attention is all you need," presented at the Proceedings of the 31st International Conference on Neural Information Processing Systems, Long Beach, California, USA, 2017.
- [12] Y. Liu, F. R. Nezami, E. R. Edelman, "A Transformer-based pyramid network for coronary calcified plaque segmentation in intravascular optical coherence tomography images," unpublished.